International Conference on Resonances in Condensed Matter: Altshuler100 IOP Publishing
Journal of Physics: Conference Series **324** (2011) 012007 doi:10.1088/1742-6596/324/1/012007

Direct and two-phonon Orbach-Aminov type spin-lattice relaxation in molecular magnet V_{15}

Alex Tarantul[1] **and Boris Tsukerblat**[1,2]

[1]Department of Chemistry, Ben-Gurion University of the Negev, 84105 Beer-Sheva, Israel

E-mail: tsuker@bgu.ac.il

Abstract. In this article we propose a model of spin-phonon relaxation in $K_6[V^{IV}{}_{15}As_6O_{42}(H_2O)]\cdot 8H_2O$, the so called V_{15} cluster exhibiting the unique layered magnetic structure. The work is motivated by the recent observation of the Rabi oscillation [1] in this system and aimed to elucidate the role of spin-phonon interaction as a source of decoherence. The spin-phonon coupling is assumed to appear as a result of the modulation of the isotropic and antisymmetric (Dzyaloshinsky-Moriya) exchange interactions in the central triangular layer of vanadium ions by the acoustic lattice vibrations. The relaxation rates are estimated within the Debye model for the lattice vibrations. Within the pseudo-angular momentum representation the selection rules for the direct (one-phonon) transitions between Zeeman levels are derived and a special role of the antisymmetric exchange is underlined. The probabilities of the two-phonon Orbach-Aminov type processes are evaluated as well, while the Raman type relaxation is shown to have a negligible importance at low temperatures at which the Rabi oscillations have been detected.

Keywords: molecular magnetism, cluster V_{15}, exchange interaction, antisymmetric exchange, spin-phonon relaxation, spin frustration, coherence/decoherence

1. Introduction

During the last two decades quantum computing became one of the most promising disciplines lying on the border of computer science, quantum physics and theory of information. The main idea is that if some quantum system has (at least) two quantum states $|1\rangle$ and $|2\rangle$, not only these two pure states may be interpreted as information storage bits "0" and "1", but any superposition of them is also a carrier of information. Unlike its classical counterpart, this quantum information unit, or quantum bit (*qubit*) possesses intrinsic parallelism due to which quantum computation promises efficient algorithms which are not realizable on the classical computers [2]. However implementation of quantum computing is threatened by the decoherence, when the memory content of a qubit is lost due to its interaction with the environment (thermal bath, intercluster interaction or/and hyperfine spin-spin coupling). In order to successfully encode and process information the time of decoherence must be sufficiently long and, at least, not shorter than duration of the gate logical operation. This statement allows mentioning the central problem in the realization of quantum

---

[2] Author to whom any correspondence should be addressed

computing: to elaborate quantum system with a long coherence time. The first quantum logic gates have been already successfully realized on the trapped cold ions [3, 4]. The microscopic spins in quantum dots [5], semiconductors [6] and doped fullerenes [7] were also intensively studied as possible qubits.

A decade ago Leuenberger and Loss [8] proposed molecular magnets as promising candidates for the use as nanoscale qubits. In this respect it is to be mentioned that molecular magnets have a number of vitally important advantages: (a) unlike quantum dots the molecular magnets of a specified chemical composition are strictly identical and therefore have *identical physical characteristics* (energy levels, g-factors, magnetic exchange parameters, etc.); (b) by a proper chemical synthesis the magnetic clusters can be *engineered* to have desired physical characteristics that can be controlled by the due choice of the metal ions, ligands, etc. Moreover, in this way the main sources of decoherence (like the dipolar coupling and spin-nuclei interaction) can be suppressed by the chemical means. [1, 9, 10]; (c) Molecular magnets are relatively large (but still nanoscale!) objects, (as compare to single ions) and thus much easier for the *individual addressing* while processing the information; (d) magnetic molecules can be attached to *different types of platforms* by grafting individual clusters on solid surfaces [11-14], grafting monolayers [15-17] or embedding the isolated molecules in the amorphous media [1, 10]. This is expected to provide a firm stable structure in opposite to fragile and expensive apparatus for ion trapping.

The key question regarding molecular magnets as possible qubits was formulated by Winpenny et al. (see [9]): “will coherence times in molecular magnets permit quantum information processing?” A number of approaches for implementation of molecular magnets as qubits were proposed [8, 18-23] and the existence of the long living coherent states in different kinds of molecular magnets [1, 9, 23-27] have been predicted. The long phase-decoherence time T_2 in the heterometallic Cr_7M wheels was reported in [9]. The understanding of the significant importance of molecular magnets as possible qubits gave a strong impact on the study of the decoherence mechanisms, especially, spin-lattice and spin-spin interactions in molecular magnets [27-31]

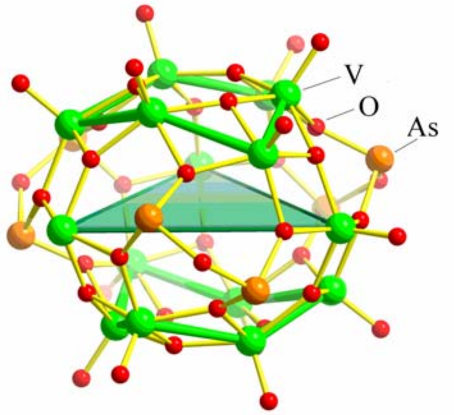

Figure 1. Ball-and-stick representation of the cluster anion $[V^{IV}{}_{15}As_6O_{42}(H_2O)]^{6-}$ emphasizing the V_3 triangle (the central water molecule is not indicated) [32].

A possibility of the long living coherent states in V_{15} have been theoretically predicted by Dobrovitski et al. [27] on the basis of the estimation of the characteristic times related to different mechanisms of decoherence. In fact, later on the existence and interpretation of the long-living coherent states was demonstrated by the first observation of the Rabi oscillations in the molecular magnet $K_6[V^{IV}{}_{15}As_6O_{42}(H_2O)]\cdot 8H_2O$, hereafter – V_{15} cluster [1].

The unique cluster V_{15} containing fifteen V^{IV} ions (S_i=1/2) and exhibiting layered structure was discovered more than two decades ago by Müller and Döring [32] and the first studies of this system date back to this period [32-35]. The metal skeleton of the V_{15} cluster has a distinct layered quasi-spherical structure [32, 33] in which fifteen magnetic V^{IV} ions ($s_i = 1/2$) are placed in a large central triangle sandwiched by two distorted hexagons possessing overall $\mathbf{D}_3$ symmetry (figure 1). The studies of the static magnetic susceptibility [34-37], energy pattern [38-43], *ab initio* electronic structure calculations [44-48] and inelastic neutron scattering [49, 50] showed that the low lying part of the energy spectrum is well isolated from the remaining spin levels and can be understood as a result of interaction between three moieties consisting of five strongly coupled spins (two almost paired spins from each hexagon coupled to a spin of the triangle) giving rise to spin S =1/2 of each moiety. The twenty-year studies of V_{15} cluster have been recently reviewed in [51].

In their study of the decoherence in molecular magnets the authors of [27] compared the dipole-dipole and spin-lattice relaxation times and according to their estimations the first was shown to be a dominant mechanism. The theory of spin-lattice relaxation in [27] had been based on a semiempirical model that led to a general estimations of some characteristic relaxation times . In this article we attempt to develop a microscopic model of spin-lattice interaction in V_{15} that takes into account isotropic and anisotropic exchange interactions and based on the accurate consideration of the spin states and Zeeman levels of V_{15} and on a simplified Debye model for the acoustic lattice vibrations. We consider direct (one-phonon) and two-phonon Raman and Orbach-Aminov type processes in order to estimate the relaxation rates and to reveal the importance of spin-phonon relaxation as a source of the decoherence in the V_{15} system.

2. Triangle model for V_{15} cluster

The model of spin triangle for the low lying spin excitations suggested in [34,35] includes the isotropic Heisenberg-Dirac-Van Vleck (HDVV) exchange interaction and the antisymmetric (AS) exchange proposed by Dzyaloshinskii [52] and Moriya [53] (see also [53-57]) as an origin of spin canting in magnetic materials. The last interaction was shown [57-62] to be especially important for the spin frustrated system possessing triangular structure. It was shown that the spin of hexagons are paired due to relatively strong antiferromagnetic interactions while the coupling inside the triangle is relatively small. That is why the model of an effective spin triangle of vanadium ions ($S = 1/2$) belonging to the central triangle provides an adequate description of the whole system at low temperatures. This triangular vanadium magnetic layer in the V_{15} structure is shaded in figure 1. Three spins of the central triangle are coupled through the antiferromagnetic isotropic exchange. The full Hamiltonian of the system in the external magnetic field looks as:

$$H \equiv H_0 + H_{AS} = 2J(\mathbf{S}_1\mathbf{S} + \mathbf{S}_2\mathbf{S}_3 + \mathbf{S}_3\mathbf{S}_1) + \sum_{i,j} \mathbf{D}_{ij}\left[\mathbf{S}_i \times \mathbf{S}_j\right] + g\mu\mathbf{SH}\,, \qquad (1)$$

where for the sake of simplicity the Zeeman interaction is assumed to be isotropic. The eigen-values of the Hamiltonian H_0 with the antiferromagnetic ($J > 0$) coupling include two levels, namely, two "accidentally" degenerate spin doublets (ground manifold) and excited spin quadruplet separated by the gap $3J$. According to the overall point symmetry $\mathbf{D}_3$ the vector constants $\boldsymbol{D}_{ij}$ ($ij = 12,23,31$ numerate the sides) of the AS exchange have, in general, three independent components: along and perpendicular to the side (in plane of the triangle) and perpendicular to the plane component whose absolute values are D_l, D_t and D_n respectively. Consequently the Hamiltonian H_{AS} can be divided into two parts, $H_{AS}(\|)$ ("normal") and $H_{AS}(\perp)$ ("in-plane") which are defined as:

$$H_{AS}(\|) = D_n\left([\boldsymbol{S}_1 \times \boldsymbol{S}_2]_Z + [\boldsymbol{S}_2 \times \boldsymbol{S}_3]_Z + [\boldsymbol{S}_3 \times \boldsymbol{S}_1]_Z\right), \tag{2}$$

$$\begin{aligned} H_{AS}(\perp) = {} & D_l\left([\boldsymbol{S}_1 \times \boldsymbol{S}_2]_X - \frac{1}{2}[\boldsymbol{S}_2 \times \boldsymbol{S}_3]_X + \frac{\sqrt{3}}{2}[\boldsymbol{S}_2 \times \boldsymbol{S}_3]_Y - \frac{1}{2}[\boldsymbol{S}_3 \times \boldsymbol{S}_1]_X - \frac{\sqrt{3}}{2}[\boldsymbol{S}_3 \times \boldsymbol{S}_1]_Y\right) \\ & + D_t\left([\boldsymbol{S}_1 \times \boldsymbol{S}_2]_Y - \frac{\sqrt{3}}{2}[\boldsymbol{S}_2 \times \boldsymbol{S}_3]_X - \frac{1}{2}[\boldsymbol{S}_2 \times \boldsymbol{S}_3]_Y + \frac{\sqrt{3}}{2}[\boldsymbol{S}_3 \times \boldsymbol{S}_1]_X - \frac{1}{2}[\boldsymbol{S}_3 \times \boldsymbol{S}_1]_Y\right) \end{aligned} \tag{3}$$

where axes X and Y of the global coordinates system are in the plane (figure 3) while the axis Z is perpendicular to the plane. These two parts of the AS exchange are explicitly separated as they play quite different physical roles. The normal part of AS exchange splits the ground $S = 1/2$ doublets into two Kramers doublets and gives rise to a strong (first order) magnetic anisotropy while the in-plane part is responsible for the doublet-quadruplet mixing. This mixing leads to the second order zero-field splitting of the $S = 3/2$ level (that is $\left(D_l^2 + D_t^2\right)/8J$). It was shown [59] that D_l and D_t are combined into an effective parameter $D_\perp = \sqrt{D_t^2 + D_l^2}$ so the exchange model is fully specified by the three parameters J, D_n and $D_\perp$ (see Section 7 for the numerical estimations).

3. EPR transitions

The analysis of the energy pattern of the system shows that the ground term is represented by the orbital doublet ${}^2E$ (S=1/2) while the excited level is the orbital singlet ${}^4A_2(S = 3/2)$. This allows to find out the selection rule for the EPR transitions and to reveal the role of the AS exchange. The

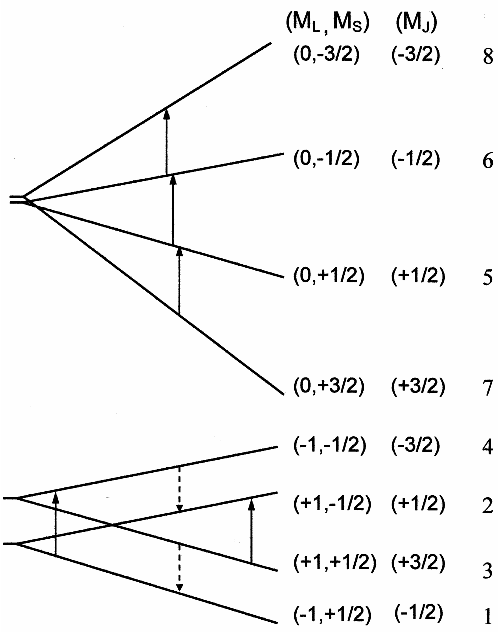

Figure 2. Allowed EPR transitions (low frequency range), $\boldsymbol{H} \,\|\, \boldsymbol{C}_3$ (solid arrows); allowed one-phonon transitions caused by the modulation of the isotropic exchange (dashed arrows), see Section 5.

component $H_{AS}(\|)$ of the AS exchange splits the ground manifold ^2E (S=1/2) while in-plane component $H_{AS}(\perp)$ of the AS exchange mixes the ground and excited levels and gives rise to a zero-field splitting of the excited $^4A_2(S=3/2)$ level. At low magnetic fields the effects of the in-plane component $H_{AS}(\perp)$ of the AS exchange are negligible due to the relatively large gap $3|J|$. Then, if the field is parallel to the $\boldsymbol{C}_3$ axis the energy levels may be labeled by following quantum numbers: the projection M_L of the orbital pseudo-angular momentum, the spin projection M_S and the full angular momentum projection $M_J = M_L + M_S$ [51,59,62]. Consequently, if $H_{AS}(\perp)$ is neglected, the EPR transitions satisfy the selection rules $\Delta M_L = 0$, $\Delta M_S = \pm 1$, $\Delta M_J = \pm 1$ [62]. There are five allowed transitions: two between the Kramers doublets and three within the excited quadruplet (figure 2). If the effects of $H_{AS}(\perp)$ are taken into account, then M_L and M_S are no longer “good” quantum numbers and the selection rule is now $\Delta M_J = \pm 1$. This allows for a number of additional EPR transitions which are, however, weak (their intensities are related to the degree of the intermultiplet mixing through the $H_{AS}(\perp)$) and may have importance only near the crossover points of the Zeeman sublevels. In terms of the quantum numbers M_L, M_S and M_J in Sec. 5 we will consider the selection rules for the one-phonon transitions.

4. Spin-phonon interaction

The interaction of spins with the lattice vibrations (heat reservoir) is assumed to arise from the modulation of the isotropic and AS exchange interactions by the molecular displacements X_i, Y_i, Z_i ($i = 1,2,3$ enumerates the ions) in course of the lattice vibrations [57, 58, 63]. It is convenient to deal with the symmetry adapted coordinates Q_α (α enumerates the vibrational mode) of the equilateral triangular unit: full symmetric $A_1(Q_{A_1} \equiv Q_A)$ and double degenerate E type $(Q_{Ex} \equiv Q_x, Q_{Ey} \equiv Q_y)$.

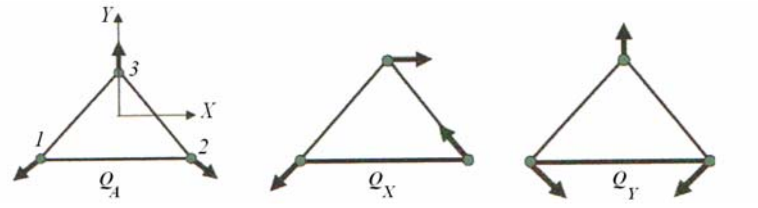

Figure 3. Vibrational coordinates of a symmetric triangular unit.

These normal coordinates can be expressed in terms of the Cartesian displacements X_i, Y_i, Z_i of the constituent ions as following:

$$
\begin{aligned}
Q_A &= \frac{1}{\sqrt{3}}\left[-\frac{1}{2}\left(\sqrt{3}X_1 + Y_1\right) + \frac{1}{2}\left(\sqrt{3}X_2 - Y_2\right) + Y_3\right] \\
Q_X &= \frac{1}{\sqrt{3}}\left[\frac{1}{2}\left(X_1 + \sqrt{3}Y_1\right) + \frac{1}{2}\left(X_2 - \sqrt{3}Y_2\right) - X_3\right] \\
Q_Y &= \frac{1}{\sqrt{3}}\left[\frac{1}{2}\left(\sqrt{3}X_1 - Y_1\right) - \frac{1}{2}\left(\sqrt{3}X_2 + Y_2\right) + Y_3\right]
\end{aligned} \qquad (4)
$$

The displacements corresponding to these coordinates are shown in figure 3. Within the mentioned mechanism of spin-phonon interaction the exchange parameters are assumed to be the functions of the metal-metal distances R_{ij} so that the linear (with respect to the displacements) terms of the vibronic Hamiltonian H_{ev} can be represented as a sum of two contributions $H_{ev} = H'_{ev} + H''_{ev}$, where H'_{ev} and H''_{ev} are related to the isotropic and AS parts of the original Hamiltonian respectively:

$$H'_{ev} = \sum_{\alpha=A,X,Y} \left(\frac{\partial H_0}{\partial Q_\alpha}\right)_{Q_\alpha=0} Q_\alpha , \tag{5}$$

$$H''_{ev} = \sum_{\alpha=A,X,Y} \left(\frac{\partial H_{AS}}{\partial Q_\alpha}\right)_{Q_\alpha=0} Q_\alpha . \tag{6}$$

After substitution of the corresponding parts of the exchange Hamiltonians one obtains the following expressions for the spin-phonon coupling operators:

$$H'_{ev} = \sum_{ij} \sum_{\alpha=A,X,Y} 2\boldsymbol{S}_i \boldsymbol{S}_j \left(\frac{\partial J_{ij}(R_{ij})}{\partial R_{ij}}\right)_{\Delta R_{ij}=0} \cdot \frac{\partial R_{ij}}{\partial Q_\alpha} Q_\alpha \tag{7}$$

$$H''_{ev} = \sum_{ij} \sum_{\alpha=A,X,Y} [\boldsymbol{S}_i \times \boldsymbol{S}_j] \left(\frac{\partial \boldsymbol{D}_{ij}(R_{ij})}{\partial R_{ij}}\right)_{\Delta R_{ij}=0} \cdot \frac{\partial R_{ij}}{\partial Q_\alpha} Q_\alpha \tag{8}$$

Here R_{ij} are the instant metal-metal distances in course of the vibrations ($\Delta R_{ij} = 0$ corresponds to the equilibrium trigonal configuration and symmetric exchange network with the sides R_0). Modulation of the isotropic exchange can be described by the parameter λ which is defined as $\lambda \equiv \sqrt{6}\left(\partial J_{ij}(R_{ij})/\partial R_{ij}\right)_0$. For each side of the triangle there is also vector coupling parameter which related to AS exchange and defined as $\boldsymbol{\beta}_{ij} = \left(\partial \boldsymbol{D}_{ij}(R_{ij})/\partial R_{ij}\right)_0$. Due to trigonal symmetry of the system the absolute values of these three vector parameters have the same value β for each side of the triangle. One can define also the three components of $\boldsymbol{\beta}_{ij}$, namely, the normal part $\beta_n = \beta_{ijn}$ and the two perpendicular contributions $\beta_t = \beta_{ijt}$ and $\beta_l = \beta_{ijl}$ where the symbols *l* and *t* have the same meaning as in the definition of the AS exchange Hamiltonian. One can also define a combined vibronic parameter $\beta_\perp = \sqrt{\beta_t^2 + \beta_l^2}$ that appears in the final results.

After calculation of the derivatives $\partial R_{ij} / \partial Q_\alpha$ (using the relations between the Cartesian displacements X_i, Y_i, Z_i and normal coordinates Q_α, figure 3) one arrives at the following form of the spin-vibronic Hamiltonians:

$$H'_{ev} = \sum_{\Gamma\gamma} \lambda \hat{V}_{\Gamma\gamma} Q_{\Gamma\gamma} ,$$
$$H''_{ev} = \sum_{\Gamma\gamma} \beta \hat{W}_{\Gamma\gamma} Q_{\Gamma\gamma} ,. \tag{9}$$

Here $\Gamma\gamma = A_1, E_X, E_Y$ label the irreducible representations and basis functions of the $\boldsymbol{D}_3$ symmetry group and the operators $\hat{V}_{\Gamma\gamma}$ (related to the isotropic part of the Hamiltonian) are expressed in terms of the scalar products of spin operators:

$$\begin{aligned}
\hat{V}_{A_1} &= \sqrt{\frac{2}{3}}\left(\boldsymbol{S}_1\boldsymbol{S}_2 + \boldsymbol{S}_2\boldsymbol{S}_3 + \boldsymbol{S}_3\boldsymbol{S}_1\right) , \\
\hat{V}_X &= \frac{1}{\sqrt{6}}\left(\boldsymbol{S}_2\boldsymbol{S}_3 + \boldsymbol{S}_3\boldsymbol{S}_1 - 2\boldsymbol{S}_1\boldsymbol{S}\right) , \\
\hat{V}_Y &= \frac{1}{\sqrt{2}}\left(\boldsymbol{S}_2\boldsymbol{S}_3 - \boldsymbol{S}_3\boldsymbol{S}_1\right) .
\end{aligned} \tag{10}$$

The operators $\hat{W}_{\Gamma\gamma}$ (related to the modulation of the AS exchange) are expressed in terms of the vector products of spin operators as follows:

$$\begin{aligned}
\hat{W}_A &= \boldsymbol{e}_{12}\left[\boldsymbol{S}_1 \times \boldsymbol{S}_2\right] + \boldsymbol{e}_{23}\left[\boldsymbol{S}_2 \times \boldsymbol{S}_3\right] + \boldsymbol{e}_{31}\left[\boldsymbol{S}_3 \times \boldsymbol{S}_1\right] , \\
\hat{W}_X &= \frac{1}{2}\left(\boldsymbol{e}_{12}\left[\boldsymbol{S}_1 \times \boldsymbol{S}_2\right] + \boldsymbol{e}_{23}\left[\boldsymbol{S}_2 \times \boldsymbol{S}_3\right] - 2\boldsymbol{e}_{31}\left[\boldsymbol{S}_3 \times \boldsymbol{S}_1\right]\right) , \\
\hat{W}_Y &= \frac{\sqrt{3}}{2}\left(\boldsymbol{e}_{23}\left[\boldsymbol{S}_2 \times \boldsymbol{S}_3\right] - \boldsymbol{e}_{31}\left[\boldsymbol{S}_3 \times \boldsymbol{S}_1\right]\right) .
\end{aligned} \tag{11}$$

where $\boldsymbol{e}_{ij}$ are the unit vectors $\boldsymbol{\beta}_{ij}/\beta_{ij}$. The evaluation of the vibronic matrices was performed with the aid of the irreducible tensor operators approach [57, 58, 64-67].

5. One-phonon relaxation

In order to take into account the interaction of spins with the acoustic lattice vibrations, the symmetry adapted molecular displacement should be expanded into series of the longitudinal (*l*) and transverse (*t*) acoustic lattice vibrational modes $q_{\boldsymbol{\kappa} p}$ specified by the wave vector $\boldsymbol{\kappa}$ and polarization $p = l, t$. We will also use a short notation $\xi = (\boldsymbol{\kappa}\, p)$ unless we have a special need to address any of them. Then one can obtain the following expression for the spin-phonon Hamiltonian:

$$H_{e\upsilon} = \sum_{\Gamma\gamma} \hat{G}_{\Gamma\gamma} \sum_{\xi} \left(\frac{\hbar}{M\omega_\xi}\right)^{1/2} a_\xi(\Gamma\gamma) q_\xi \tag{12}$$

Here the matrix $\hat{G}_{\Gamma\gamma}$ is defined as $\hat{G}_{\Gamma\gamma} = \lambda\hat{V}_{\Gamma\gamma} + \beta\hat{W}_{\Gamma\gamma}$, q_ξ are the dimensionless normal coordinates of the lattice, M is a mass of crystal and $a_\xi(\Gamma\gamma)$ are the so called Van Vleck coefficients introduced in his underlying theory of paramagnetic relaxation [68].

Since we are dealing with the transitions between the levels belonging to the ground manifold of V_{15} separated by the gaps of a few cm^{-1}, (Section 7) it is sufficient to use the long-wave approximation for the Van Vleck coefficients of the triangular unit:

$$\begin{aligned} a_{\boldsymbol{\kappa}}(A_1) &= (1/2)R_0\left(p_x\kappa_x + p_y\kappa_y\right) \\ a_{\boldsymbol{\kappa}}(E_X) &= -(1/2)R_0\left(p_x\kappa_x - p_y\kappa_y\right) \\ a_{\boldsymbol{\kappa}}(E_Y) &= -(1/2)R_0\left(p_x\kappa_y - p_y\kappa_x\right) \end{aligned} \tag{13}$$

where κ_i, p_i are Cartesian components of the wave-vector and polarization vector and R_0 is V-V distance in the vanadium triangle. It is to be noted that the spin-phonon Hamiltonian, Eq. (12), is adapted to the triangle model for V_{15}. In fact, by definition the matrices $\hat{G}_{\Gamma\gamma}$ in this Hamiltonian act within the set of eight spin functions (two $S = 1/2$ doublets and quadruplet $S = 3/2$) of the vanadium triangle.

In the case of two non-degenerate electronic states $|m'\rangle$ and $|m\rangle$ separated by the energy gap $\Delta E = E_m - E_{m'} > 0$ the probability of the one-phonon transition $|m\rangle \to |m'\rangle$ is given by

$$w_\sigma = \frac{2\pi}{\hbar}\overline{\left|\langle m,n|H_{e\upsilon}|m',n'\rangle\right|^2}\,\delta(\hbar\omega - \Delta E) \tag{14}$$

where $|n\rangle = |....,n_\sigma,.....\rangle$ and $|n'\rangle = |....,n_\sigma \pm 1,.....\rangle$. Using equation (12) for the spin-vibronic Hamiltonian one sees that the matrix element in (14) is the following:

$$\langle m,n|H_{e\upsilon}|m',n'\rangle = \sum_{\Gamma\gamma}\sum_{\xi}\left(\frac{\hbar}{M\omega_\xi}\right)^{1/2} a_\xi(\Gamma\gamma)\langle m|\hat{G}_{\Gamma\gamma}|m'\rangle\langle n_\sigma|q_\xi|n_\sigma \pm 1\rangle \tag{15}$$

The squared Van Vleck coefficients $b^2_{\kappa p}(\Gamma) = \overline{a^2_{\boldsymbol{\kappa} p}(\Gamma\gamma)}$ averaged over polarization directions and directions of the wave-vectors are found as

$$\begin{aligned} b^2_{\kappa l}(A_1) &= \frac{2}{15}\kappa^2 R_0^2 \quad , \quad b^2_{\kappa l}(E) = \frac{1}{15}\kappa^2 R_0^2 \\ b^2_{\kappa t}(A_1) &= \frac{1}{60}\kappa^2 R_0^2 \quad , \quad b^2_{\kappa t}(E) = \frac{1}{20}\kappa^2 R_0^2 \end{aligned} \tag{16}$$

We use also a short notation:

$$b^2_\kappa(\Gamma) = b^2_{\kappa l}(\Gamma) + b^2_{\kappa t}(\Gamma) \tag{17}$$

Using the expression for the density of states $f(\omega) = \frac{V\omega^2}{(2\pi)^2\upsilon^3}$ (V is the volume of crystal, υ is the mean sound velocity) and orthogonality of the Van Vleck coefficients one obtains the full probability $w^{(1)}_{m\to m'}$ of system's transition from $|m'\rangle$ to $|m\rangle$ with emission of a phonon of the resonance frequency $\omega = \Delta E/\hbar$:

$$w^{(1)}_{m\to m'} = \frac{\omega}{\pi\hbar\rho\upsilon^3}\,\frac{exp(\hbar\omega/kT)}{exp(\hbar\omega/kT) - 1}\left(\sum_\Gamma b^2_\kappa(\Gamma)\sum_\gamma\left|\langle m|\hat{G}_{\Gamma\gamma}|m'\rangle\right|^2\right) \tag{18}$$

where ρ is a crystal density and $\kappa = \omega/\upsilon = \Delta E/\hbar\upsilon$ in the long-wave approximation so far employed. Using equations (16) and (17) one arrives at the following result which is specific just for a triangular unit:

$$w^{(1)}_{m\to m'} = \frac{R_0^2}{\pi\hbar\rho\upsilon^5}\,\frac{\exp(\hbar\omega/kT)}{\exp(\hbar\omega/kT)-1}\,\omega^3 B_{mm'}, \tag{19}$$

where

$$B_{mm'} = \frac{3}{20}\left|\langle m|\hat{G}_A|m'\rangle\right|^2 + \frac{7}{60}\left|\langle m|\hat{G}_X|m'\rangle\right|^2 + \frac{7}{60}\left|\langle m|\hat{G}_Y|m'\rangle\right|^2 \tag{20}$$

The one-phonon relaxation time is thus:

$$1/\tau_D = w_{m'\to m} + w_{m\to m'}\ .$$

If the in-plane part $H_{AS}(\perp)$ of AS interaction is neglected, the eigen-functions are given by the vectors $\boldsymbol{e}_i$, $i = 1,\cdots,8$, specified by the spin-projection M_S as well as by the pseudo-angular momentum quantum numbers M_L and M_J (Section 3). This vector set can be referred to as "pure" basis (Appendix). The $H_{AS}(\perp)$ part of the Hamiltonian causes mixing of the "pure" basis vectors that is quite negligible except of the levels crossover fields [51,59-62]. The matrix $\boldsymbol{B}$ in the "pure" basis is given in Appendix. The entries of matrix $\boldsymbol{B}$ in the "pure" basis refer to the strongest direct transitions which will be referred to as "first type" transitions.

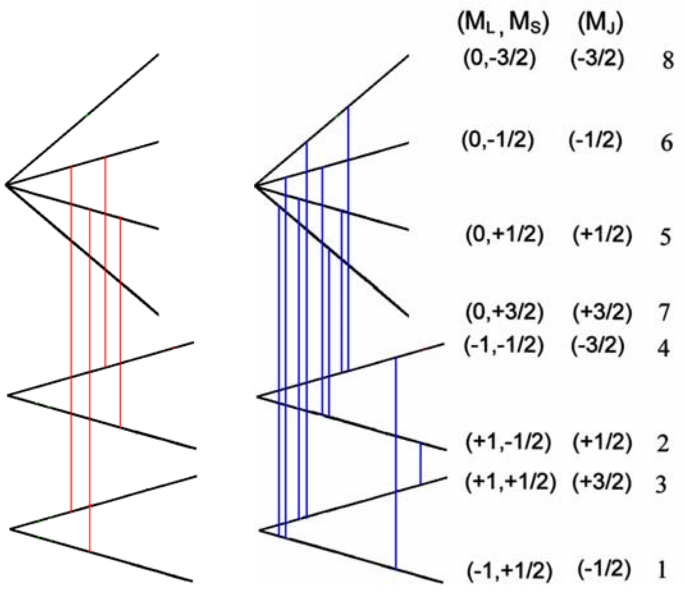

Figure 4. One phonon transitions caused by the phonon modulation of the normal part of the AS-exchange (left) and in-plane AS-exchange (right), $\boldsymbol{H} \,||\, \boldsymbol{C}_3$.

Most of the first type transitions originate from the phonon-modulated AS exchange rather then from the modulated isotropic interaction. Indeed the modulation of the isotropic exchange produces only two first-type transitions within the $S = 1/2$ manifold (figure 2); these transitions obey the selection rules $\Delta M_S = 0, \Delta M_J = \pm 2$. Selection rules for the first-type transitions emerging from the acoustic modulation of the normal AS exchange component $H_{AS}(\|)$ are: $\Delta M_L = \pm 1,\ \Delta M_S = 0,\ \Delta M_J = \pm 1$ (figure 4, left). First-type transitions emerging from the acoustic modulation of the in-plane AS exchange component $H_{AS}(\perp)$ are shown in the figure 4, right. One can see that the most of the transitions originate from the spin modulation of the components of AS exchange rather then modulation of the isotropic exchange. Another important observation is that the first-type transitions within the $S = 3/2$ quadruplet are forbidden.

When the level mixing by the in-plane AS exchange Hamiltonian $H_{AS}(\perp)$ is taken into consideration, the M_L and M_S are no longer "good" quantum numbers and the selection rules should be formulated in terms of the total angular momentum projection M_J. Then the selection rules for the acoustically modulated isotropic exchange is now $\Delta M_J = \pm 2$ (quadrupole type of transitions) and for the modulated normal component $H_{AS}(\|)$ is $\Delta M_J = \pm 1$ (dipole type transitions). Selection rules for the modulated in-plane component $H_{AS}(\perp)$ become also less strict. This gives rise to emergence of additional very weak "second type" transitions whose probability is at least two orders smaller then that for the first-type relaxations.

6. Two phonon Orbach-Aminov relaxation

Since in the one-phonon transitions the density of the phonon states at the resonance frequencies is small, an important rule play the two-phonon relaxation processes. These are the Raman processes and the Orbach-Aminov type processes [69-73]. Due to the fact that the excited levels corresponding to the unpaired spins of the hexagons in V_{15} are higher then the Debye energy, the levels of the central vanadium triangle contribute significantly to the second order relaxation. That is why one can expect that only the resonant Orbach-Aminov type relaxation is actual for the V_{15} system at the relatively low temperatures corresponding to the actual EPR measurements. The Raman processes become important only at high temperatures. Later on we will derive general expressions adapted to the V_{15} system.

Let us consider now the two-step relaxation process in which the system passes from the initial state $|m,n\rangle$ to the final state $|m',n'\rangle$ through the intermediate state $|j,n''\rangle$. The probability of this two-stage transition is given in the framework of second-order perturbation theory (see, for example, [69]) by:

$$w_{\sigma_1,\sigma_2} = \frac{2\pi}{\hbar}\overline{\left|\sum_{j,n''}\frac{\langle m,n|H_{ev}|j,n''\rangle\langle j,n''|H_{ev}|m',n'\rangle}{E_m + E_n - E_j - E_{n''}}\right|^2}\,\delta\left(E_m + \hbar\omega_2 - E_{m'} - \hbar\omega_1\right) \tag{21}$$

Using the notation $\Delta_j = E_j - E_m$, the complex matrix element can be presented as:

$$\sum_{j,n}\frac{\langle m,n|H_{ev}|j,n''\rangle\langle j,n''|H_{ev}|m',n'\rangle}{E_m+E_n-E_j-E_{n''}}=$$
$$\sum_{j}\{\sum_{\Gamma\gamma,\xi}c(\xi)a_{\xi}(\Gamma\gamma)\langle m|G_{\Gamma\gamma}|j\rangle\langle n_{\sigma_1}|q_{\xi}|n_{\sigma_1}+1\rangle\frac{\sum\limits_{\Gamma'\gamma'\xi'}c(\xi')a_{\xi'}(\Gamma'\gamma')\langle j|G_{\Gamma'\gamma'}|m'\rangle\langle n_{\sigma_2}|q_{\xi'}|n_{\sigma_2}-1\rangle}{-\hbar\omega_1-\Delta_j}$$
$$+\sum_{\Gamma\gamma,\xi}c(\xi)a_{\xi}(\Gamma\gamma)\langle m|G_{\Gamma\gamma}|i\rangle\langle n_{\sigma_2}|q_{\xi}|n_{\sigma_2}-1\rangle\frac{\sum\limits_{\Gamma'\gamma'\xi'}c(\xi')a_{\xi'}(\Gamma'\gamma')\langle j|G_{\Gamma'\gamma'}|m'\rangle\langle n_{\sigma_1}|q_{\xi'}|n_{\sigma_1}+1\rangle}{\hbar\omega_2-\Delta_j}\} \tag{22}$$

where $c(\xi)=(\hbar/M\omega_{\xi})^{1/2}$. After deriving the expression for the squared matrix element, using the orthogonality properties of Van Vleck coefficients and performing thermal averaging one obtains:

$$\overline{\left|\sum_{j,n''}\frac{\langle m,n|H_{ev}|j,n''\rangle\langle j,n''|H_{ev}|m',n'\rangle}{E_m+E_n-E_j-E_{n''}}\right|^2}$$
$$=\frac{\hbar^2}{M^2\omega_1\omega_2}\cdot\frac{\exp(\hbar\omega_1/kT)}{(\exp(\hbar\omega_1/kT)-1)(\exp(\hbar\omega_2/kT)-1)}$$
$$\times\sum_{j,j'}\left\{\left(\sum_{\Gamma}b^2_{\kappa_1}(\Gamma)\sum_{\gamma}\langle m|G_{\Gamma\gamma}|j\rangle\langle m|G_{\Gamma\gamma}|j'\rangle\right)\cdot\frac{\left(\sum\limits_{\Gamma}b^2_{k_2}(\Gamma)\sum\limits_{\gamma}\langle j|G_{\Gamma\gamma}|m'\rangle\langle j'|G_{\Gamma\gamma}|m'\rangle\right)}{(\hbar\omega_1+\Delta_j)(\hbar\omega_1+\Delta_{j'})}\right.$$
$$+\left(\sum_{\Gamma}b^2_{\kappa_1}(\Gamma)\sum_{\gamma}\langle j|G_{\Gamma\gamma}|m'\rangle\langle j'|G_{\Gamma\gamma}|m'\rangle\right)\cdot\frac{\left(\sum\limits_{\Gamma}b^2_{k_2}(\Gamma)\sum\limits_{\gamma}\langle m|G_{\Gamma\gamma}|j\rangle\langle m|G_{\Gamma\gamma}|j'\rangle\right)}{(\hbar\omega_2-\Delta_j)(\hbar\omega_2-\Delta_{j'})}$$
$$-\left(\sum_{\Gamma}b^2_{\kappa_1}(\Gamma)\sum_{\gamma}\langle m|G_{\Gamma\gamma}|j\rangle\langle j'|G_{\Gamma\gamma}|m'\rangle\right)\cdot\frac{\left(\sum\limits_{\Gamma}b^2_{k_2}(\Gamma)\sum\limits_{\gamma}\langle j|G_{\Gamma\gamma}|m'\rangle\langle m|G_{\Gamma\gamma}|j'\rangle\right)}{(\hbar\omega_1+\Delta_j)(\hbar\omega_2-\Delta_{j'})}$$
$$\left.-\left(\sum_{\Gamma}b^2_{\kappa_1}(\Gamma)\sum_{\gamma}\langle j|G_{\Gamma\gamma}|m'\rangle\langle m|G_{\Gamma\gamma}|j'\rangle\right)\cdot\frac{\left(\sum\limits_{\Gamma}b^2_{k_2}(\Gamma)\sum\limits_{\gamma}\langle m|G_{\Gamma\gamma}|j\rangle\langle j'|G_{\Gamma\gamma}|m'\rangle\right)}{(\hbar\omega_1+\Delta_{j'})(\hbar\omega_2-\Delta_j)}\right\} \tag{23}$$

Without lack of generality let us suppose that all intermediate levels are situated above the states $|m\rangle$, $|m'\rangle$ so that all parameters Δ_j are assumed to be positive. The probability of two-phonon transition should be considered in two different cases.

For the levels whose Δ_j is larger then $\hbar\omega_m$ (where ω_m is the maximal Debye frequency) we encounter the Raman process and the probability should be calculated by the integration of the matrix element given by equation (23) over all frequencies above ω_m. The resonance case when $\Delta_j < \hbar\omega_m$ requires a special consideration. This important advancement in the theory of paramagnetic relaxation was made within the frame of the general theory of resonant fluorescence [74] by Orbach [70] and Aminov [71-73] (see books of Altshuler and Kozyrev [69] and Aminov and Malkin [73]). In [73] the equation was given which allows to calculate the Orbach-Aminov relaxation times τ_R in a multilevel system in terms of the one-phonon relaxation probabilities. We adopt here this equation assuming that m and m' are the labels for the initial and final states while j numerates the intermediate levels :

$$\frac{1}{\tau_R} = \frac{1}{\tau_D} + \sum_j \frac{w^{(1)}_{m\to j} w^{(1)}_{j\to m'} + w^{(1)}_{m'\to j} w^{(1)}_{j\to m}}{w^{(1)}_{j\to m} + w^{(1)}_{j\to m'}} \tag{24}$$

Equation (24) contains contributions to the overall relaxation time arising from the direct one-phonon processes (first term) that have been evaluated in Section 5 as well as the contributions from the two-phonon resonance processes.

7. Numerical estimations

The parameter J was found to be about $0.85\,cm^{-1}$ [55] and the best fit to the low temperature stepwise magnetization data [55] provided the values of $D_\perp = 0.24\,cm^{-1}$, $D_n = 0.08\,cm^{-1}$ for the parameters of the AS exchange [60, 61]. The estimations for the spin-phonon coupling constants are: $\lambda = -3\,cm^{-1}/\text{Å}$, $\beta_n \approx -0.11\,cm^{-1}/\text{Å}$, $\beta_\perp \approx -0.34\,cm^{-1}/\text{Å}$ (see refs. [51, 75]). From the X-ray data one finds the parameters $R_0 = 7\,\overset{0}{A}$ for the side of the inner triangle in V_{15} and $\rho = 3\cdot 10^3\,kg/m^3$ for the density of V_{15} [76]. The sound velocity (both transversal and longitudinal) is assumed to be $\upsilon = 2\cdot 10^3\ m/s$.

The estimated one-phonon and Orbach-Aminov relaxation times for the five most intense EPR transitions (figure 2) at the frequency $h\nu = 0.3\ cm^{-1}\ (\nu = 9\,GHz)$ in parallel field and at different temperatures are given in the Table 1.

Table 1. Relaxation times in the direct and Orbach-Aminov transitions at the frequency of 9 GHz and at different temperatures. Symbol * is related to almost forbidden one-phonon transitions (τ_D is of the order of tens of seconds).

T = 1 K				T = 5 K				T = 10 K			
m	m'	τ_D, s	τ_R, s	m	m'	τ_D, s	τ_R, s	m	m'	τ_D, s	τ_R, s
4	1	$1.3\cdot10^{-1}$	$1\cdot10^{-1}$	4	1	$3\cdot10^{-2}$	$8.3\cdot10^{-3}$	4	1	$1.5\cdot10^{-2}$	$4.1\cdot10^{-3}$
2	3	$1.5\cdot10^{-1}$	$1.1\cdot10^{-1}$	2	3	$2.7\cdot10^{-2}$	$7.8\cdot10^{-3}$	2	3	$1.4\cdot10^{-2}$	$3.4\cdot10^{-3}$
8	6	*	$2.2\cdot10^{-2}$	8	6	*	$3.8\cdot10^{-3}$	8	6	*	$3.3\cdot10^{-3}$
6	5	*	$3.5\cdot10^{-2}$	6	5	*	$5.1\cdot10^{-3}$	6	5	*	$3.9\cdot10^{-3}$
5	7	*	$2.2\cdot10^{-2}$	5	7	*	$4.6\cdot10^{-3}$	5	7	*	$2.7\cdot10^{-3}$

At $1K$ for both the one-phonon and Orbach-Aminov processes the relaxation times are of the order of $10^{-1}\,s$ within the $S = 1/2$ manifold while for the excited $S = 3/2$ manifold the direct processes show very long relaxation times of the order of tens of seconds (note, that this estimation in [75] contains an error). In this manifold Orbach-Aminov processes are much faster ($\tau_R \sim 10^{-2}\,s$). At higher temperatures Orbach-Aminov mechanism becomes the leading one in the ground manifold as well while the one-phonon processes are less significant. At these temperatures in both manifolds the Orbach-Aminov relaxation times are of the order of $10^{-3}\,s$. The relaxation times so far estimated are two orders longer then the coherence time of $1.8 \cdot 10^{-5}\, s$ measured in the Rabi oscillation experiment [1]. These estimations lead to the conclusion that the decoherence in this system can be probably attributed to the dipolar and hyperfine interactions.

8. Conclusions

In this paper we propose a model of spin-phonon relaxation in the V_{15} system that is the first molecular magnet exhibiting Rabi oscillations. It is assumed that spin-phonon interaction arises from the modulation of the isotropic and AS exchange interactions by the acoustic modes of the crystal lattice. Two mechanisms of the spin-lattice relaxations are considered, namely, the direct one-phonon relaxation and the two-phonon Orbach-Aminov mechanism within which the set of closely spaced levels of the system belonging to the central magnetic triangle act as intermediate levels. In terms of the pseudo-angular momentum representation we indicate the selection rules for the direct one-phonon processes. A special role of the different components of the AS exchange is emphasized. Most of the direct transitions arise from acoustic modulation of the AS exchange rather then from modulation of the isotropic exchange. Two phonon relaxation trajectories would not be realized if AS exchange was not present in the system.

The numerical estimations within the long-wave approximation for the acoustic vibrations show that at $1K$ for both the one-phonon and Orbach-Aminov processes the relaxation times are of the order of $10^{-1}\, s$ within the $S = 1/2$ manifold while for the excited $S = 3/2$ manifold the direct processes are inactive. In this manifold Orbach-Aminov processes are much faster ($\tau_R \sim 10^{-2}\, s$). At higher temperatures Orbach-Aminov mechanism becomes the leading one in the ground manifold as well while the one-phonon processes are less significant. At these temperatures in both manifolds the Orbach-Aminov relaxation times are of the order of $10^{-3}\, s$. The spin-phonon relaxation times prove to be two orders longer then the coherence time measured in the Rabi oscillation experiment for V_{15}.

To put the results into the perspective the following remarks are to be done. The second (after V_{15}) molecular magnet where coherent Rabi oscillations have been observed is the so called Fe_4 complex [10]. Spin-lattice relaxation time T_1 has been measured for this system and was found to be of the order of $10^{-6}\, s$. Due to its strong temperature dependence, T_1 in Fe_4 was attributed to the two-phonon processes, either Raman or Orbach-Aminov types. Since spin-lattice relaxation time has not been measured for V_{15}, and in this view it would be interesting to compare the results for two systems so far mentioned. One can rudely estimate that the isotropic spin-phonon coupling parameters λ in V_{15} and Fe_4 relate to each other as 1:10, as the isotropic constants J_0 relate ($0.85\, cm^{-1}$ in V_{15}, $8.2\, cm^{-1}$ in Fe_4 [77]). Spin-lattice relaxation times then should relate to each other as squared reciprocal values $\left(1/\lambda^2\right)$ and one may expect the order of $10^{-4}\, s$ for T_1 in V_{15}. However, since the ground state spins also relate as 1:10 ($1/2$ in V_{15}, 5 in Fe_4), relaxation rates in V_{15} may turn out to be significantly longer then even $10^{-4}\, s$ and reach the values estimated in this work.

Vanadium cluster is known for its very small spin-vibronic interaction. However, in the trinuclear low-spin systems similar to V_{15} but with strong spin-vibronic coupling (like copper cluster [78,79]) the phonon assisted relaxation is expected to be much faster, especially when the main decoherence mechanism, spin-to nuclei and dipole-dipole interactions, are substantially suppressed. According to [1] the coherence time may be increased up to $10^{-4}\, s$ when the main decoherence mechanisms are suppressed by the chemical means. The approach so far developed can be applied to more complicated spin-frustrated systems, like high-nuclearity magnetic polyoxometalates [80].

Acknowledgment

This work is done under the auspices of the Israel Science Foundation (ISF) whose financial support is gratefully acknowledged (grant no. 168/09).

Appendix

The vectors $\boldsymbol{e}_i$, $i=1,\cdots,8$ are related to the eigen-vectors in the spin coupling scheme $\left|(S_{12})SM\right\rangle$ (see [51,59]) by the following relations:

$$\boldsymbol{e}_1=\frac{1}{\sqrt{2}}\left|(0)\frac{1}{2},\frac{1}{2}\right\rangle-\frac{i}{\sqrt{2}}\left|(1)\frac{1}{2},\frac{1}{2}\right\rangle,$$

$$\boldsymbol{e}_2=-\frac{i}{\sqrt{2}}\left|(0)\frac{1}{2},-\frac{1}{2}\right\rangle+\frac{1}{\sqrt{2}}\left|(1)\frac{1}{2},-\frac{1}{2}\right\rangle,$$

$$\boldsymbol{e}_3=\frac{1}{\sqrt{2}}\left|(0)\frac{1}{2},\frac{1}{2}\right\rangle+\frac{i}{\sqrt{2}}\left|(1)\frac{1}{2},\frac{1}{2}\right\rangle,$$

$$\boldsymbol{e}_4=\frac{i}{\sqrt{2}}\left|(0)\frac{1}{2},-\frac{1}{2}\right\rangle+\frac{1}{\sqrt{2}}\left|(1)\frac{1}{2},-\frac{1}{2}\right\rangle,$$

$$\boldsymbol{e}_5=\left|(1)\frac{3}{2},\frac{1}{2}\right\rangle,\ \boldsymbol{e}_6=\left|(1)\frac{3}{2},-\frac{1}{2}\right\rangle,$$

$$\boldsymbol{e}_7=\left|(1)\frac{3}{2},\frac{3}{2}\right\rangle,\ \boldsymbol{e}_8=\left|(1)\frac{3}{2},-\frac{3}{2}\right\rangle$$

The matrix $\boldsymbol{B}$ (Section 5) in the "pure" basis $\boldsymbol{e}_i$ ($i=1,\cdots,8$) is the following:

$$\boldsymbol{B}=\frac{1}{60}\left(\begin{array}{cccc|cccc}
0 & 0 & \frac{21}{4}\lambda^2 & \frac{21}{8}\beta_\perp^2 & \frac{21}{8}\beta_n^2 & \frac{27}{16}\beta_\perp^2 & \frac{63}{32}\beta_\perp^2 & 0 \\
0 & 0 & \frac{21}{8}\beta_\perp^2 & \frac{21}{4}\lambda^2 & \frac{27}{16}\beta_\perp^2 & \frac{21}{8}\beta_n^2 & 0 & \frac{63}{32}\beta_\perp^2 \\
\frac{21}{4}\lambda^2 & \frac{21}{8}\beta_\perp^2 & 0 & 0 & \frac{21}{8}\beta_n^2 & \frac{21}{32}\beta_\perp^2 & \frac{81}{16}\beta_\perp^2 & 0 \\
\frac{21}{8}\beta_\perp^2 & \frac{21}{4}\lambda^2 & 0 & 0 & \frac{21}{32}\beta_\perp^2 & \frac{21}{8}\beta_n^2 & 0 & \frac{81}{16}\beta_\perp^2 \\
\hline
\frac{21}{8}\beta_n^2 & \frac{27}{16}\beta_\perp^2 & \frac{21}{8}\beta_n^2 & \frac{21}{32}\beta_\perp^2 & 0 & 0 & 0 & 0 \\
\frac{27}{16}\beta_\perp^2 & \frac{21}{8}\beta_n^2 & \frac{21}{32}\beta_\perp^2 & \frac{21}{8}\beta_n^2 & 0 & 0 & 0 & 0 \\
\frac{63}{32}\beta_\perp^2 & 0 & \frac{81}{16}\beta_\perp^2 & 0 & 0 & 0 & 0 & 0 \\
0 & \frac{63}{32}\beta_\perp^2 & 0 & \frac{81}{16}\beta_\perp^2 & 0 & 0 & 0 & 0
\end{array}\right)$$

References

[1] Bertaina S, Gambarelli S, Mitra T, Tsukerblat B, Müller A and Barbara B 2008 *Nature* **453**

203-207
[2] Nielsen M and Chuang I L 2000 *Quantum Computation and Quantum Information* (Cambridge: Cambridge University Press)
[3] Leibfried D, DeMarco B, Meyer V, Lucas D, Barrett M, Britton J, Itano W M, Jelenković B, Langer C, Rosenband T and Wineland D J 2003 *Nature* **422** 412-415
[4] Schmidt-Kaler F, Häffner H, Riebe M, Gulde S, Lancaster G P T, Deuschle T, Becher C, Roos C F, Eschner J and Blatt R 2003 *Nature* **422** 408-411
[5] Loss D and DiVincenzo D P 1998 *Phys. Rev. A* **57** 120-126
[6] Kane B E 1998 *Nature* **393** 133-137
[7] Morton J J L 2006 *Nature Phys.* **2** 365-366
[8] Leuenberger M N and Loss D 2001 *Nature* **410** 789-793
[9] Ardavan A, Rival O, Morton J J L, Blundell S, Tyryshkin A M, Timco G A and Winpenny R E P 2007 *Phys. Rev. Lett.* **98** 057201
[10] Schlegel C, van Slageren J, Manoli M, Brechin E K and Dressel M 2008 *Phys. Rev. Lett.* **101** 147203
[11] Zobbi L, Mannini M, Pacchioni M, Chastanet G, Bonacchi D, Zanardi C, Biagi R, del Pennino U, Gatteschi D, Cornia A and Sessoli R 2005 *Chem. Commun.* 1640-42
[12] Condorelli G G, Motta A, Fragalà I L, Giannazzo F, Raineri V, Caneschi A and Gatteschi D 2004 *Angew. Chem. Int. Ed.* **43** 4081-84
[13] Coronado E, Forment-Aliaga A, Romero F M, Corradini V, Biagi R, De Renzi V, Gambardella A and del Pennino **2005** *Inorg. Chem.* 7693-95
[14] Corradini V, Biagi R, del Pennino U, De Renzi V, Gambardella A, Affronte M, Muryn C A, Timco G A and Winpenny R E P 2007 *Inorg. Chem.* **46** 4937-43
[15] Cornia A, Fabretti A C, Pacchioni M, Zobbi L, Bonacchi D, Caneschi A, Gatteschi D, Biagi R, del Pennino U, De Renzi V, Gurevich L and Van der Zant H S J 2003 *Angew. Chem. Int. Ed.* **42** 1645-48
[16] Fleury B, Catala L, Huc V, David C, Zhong W Z, Jegou P, Baraton L, Albouy P-A and Mallah T 2005 *Chem. Commun.* 2020-22
[17] Salman Z, Chow K H, Miller R I, Morello A, Parolin T J, Hossain M D, Keeler T A, Levy C D P, MacFarlane W A, Morris G D, Saadaoui H, Wang D, Sessoli R, Condorelli GG and Kiefl R F 2007 *Nano Lett.* **7** 1551-55
[18] Troiani F, Ghirri A, Affronte M, Carretta S, Santini P, Amoretti G, Piligkos S, Timco G and Winpenny R E P 2005 *Phys. Rev. Lett.* **94** 207208
[19] Affronte M, Troiani F, Ghirri A, Carretta S, Santini P, Corradini V, Schuecker R, Muryn C, Timco G and Winpenny R E P 2006 *Dalton Trans.* 2810-17
[20] Affronte M, Troiani F, Ghirri A, Candini A, Evangelisti M, Corradini V, Carretta S, Santini P, Amoretti G, Tuna F, Timco G and Winpenny R E P 2007 *J.Phys.D: Appl.Phys* **40** 2999-3004
[21] Carretta S, Santini P, Amoretti G, Troiani F and Affronte M 2007 *Phys. Rev. B* 76 024408
[22] Stepanenko D, Trif M and Loss D 2008 *Inorg. Chim. Acta* **361** 3740-45
[23] Lehmann J, Gaita-Arino A, Coronado E and Loss D 2007 *Nature Nanotechnology* **2** 312-317
[24] Winpenny R E P 2008 *Angew. Chem. Int. Ed.* **47** 2–5
[25] Braun-Sand S B and Wiest O 2003 *J. Phys. Chem.*A **107** 285-291
[26] Morello A, Stamp P C E and Tupitsyn I S 2006 *Phys. Rev. Lett.* **97** 207206
[27] Dobrovitski V V, Katsnelson M I and Harmon B N 2000 *Phys. Rev. Lett.* **84** 3458-61
[28] Chudnovsky E M, Garanin D A and Schilling R 2005 *Phys. Rev.* B **72** 094426
[29] Mitrikas G, Sanakis Y, Raptopoulou C P, Kordas and G Papavassiliou G, 2008 *Phys. Chem. Chem. Phys*. **10** 743–748
[30] Georgopoulou A N, Sanakis Y and Boudalis A K 2011 *Dalton Trans.* **40** 6371-74
[31] Baibekov E I 2011 *JETP Lett.* **93** 292-297
[32] Müller A and Döring J 1988 *Angew. Chem. Int. Ed. Engl* **27** 1719 -21

[33] Gatteschi D, Pardi L, Barra A-L, Müller A and Döring J 1991 *Nature* **354** 463-465

[34] Barra A-L, Gatteschi D, Pardi L, Müller A and Döring J 1992 *J. Am. Chem. Soc.* **114** 8509-14

[35] Gatteschi D, Pardi L, Barra A-L and Müller A 1993 *Mol. Eng.* **3** 157

[36] Platonov V V, Tatsenko O M, Plis V I, Zvezdin A K and Barbara B 2002 *Physics of the Solid State (Rus. Fizika Tverdogo Tela)* **44** 2104-2106

[37] Kostyuchenko V V and Popov A I 2008 *J. Exp. Theor. Phys.* **107(4)** 595-602

[38] Raghu C, Rudra I, Sen D and Ramasesha S 2001 *Phys. Rev. B* **64** 064419

[39] Miyashita S, De Raedt H and Michielsen K 2003 *Prog. Theor. Phys.* **110** 889-899

[40] De Raedt H, Miyashita S, Michielsen K and Machida M 2004 *Phys. Rev. B* **70** 064401

[41] De Raedt H, Miyashita S, Michielsen K and Machida M 2004 *Phys. Stat. Solidi (b)* **241** 1180

[42] Konstantinidis N P and Coffey D 2002 *Phys. Rev. B* **66** 174426

[43] Machida M and Miyashita S 2005 *Physica E* **29** 538-540

[44] Kortus J, Pederson M R, Hellberg C S and Khanna S N 2001 *Eur. Phys. J.* D **16** 177-180

[45] Kortus J, Hellberg C S and Pederson M R 2001 *Phys. Rev. Lett.* **86** 3400

[46] Boukhvalov D W, Kurmaev E Z, Moiwes A, Zatsepin D A, Cherkashenko V M, Nemnonov S N, Finkelstein L D, Yarmoshenko Yu M, Neumann M, Dobrovitski V V, Katsnelson M I, Lichtenstein A I, Harmon B N and Koegerler P 2003 *Phys. Rev. B* **67** 134408

[47] Boukhvalov D W, Dobrovitski V V, Katsnelson M I, Lichtenstein A I, Harmon B N and Kögerler P 2004 *Phys. Rev. B* **70** 054417

[48] Barbour A, Luttrell R D, Choi J, Musfeldt J L, Zipse D, Dalal N S, Boukhvalov D W, Dobrovitski V V, Katsnelson M I, Lichtenstein A I, Harmon B N and Kögerler P 2006 *Phys. Rev. B* **74** 014411

[49] Chaboussant G, Basler R, Sieber A, Ochsenbein S T, Desmedt A, Lechner R E, Telling M T F, Kögerler P, Müller and Güdel H-U 2002 *Europhys. Lett.* **59** 291-297

[50] Chaboussant G, Ochsenbein S T, Sieber A, Güdel H-U, Mutka H, Müller A and Barbara B 2004 *Europhys. Lett.* **66** 423-429

[51] Tsukerblat B and Tarantul A 2011, The nanoscopic V_{15} cluster: a unique magnetic polyoxometalate, in *Molecular Cluster Magnets* , Ed: Winpenny R E P (Singapore: World Scientific Publishers) Ch. 3, pp. 106-180 (in press)

[52] Dzyaloshinskii I E 1957 *Sov. Phys. JETP* **5** 1259

[53] Moriya T 1960 *Phys. Rev. B* **120** 91–98

[54] Chiorescu I, Wernsdorfer W , Müller A and Bögge H 2000 *Phys. Rev. Lett.* **84** 3454

[55] Barbara B 2003 *J. Mol. Struct.* **656** 135-140

[56] Chiorescu I, Wernsdorfer W, Müller A, Bögge H and Barbara B 2000 *J.Magn. Magn. Mater.* **221** 103-109

[57] Tsukerblat B S and Belinskii M I 1983 *Magnetochemistry and Radiospectroscopy of Exchange Clusters (Russian)* (Kishinev: Stiintsa)

[58] Tsukerblat B S, Belinskii M I and Fainzilberg V E 1987 *Magnetochemistry and Spectroscopy of Transition Metal Exchange Clusters*, in *Soviet Sci. Rev. B*, M, Harwood Acad. Pub, New York, Vol**. 9** pp 337- 481

[59] Tsukerblat B, Tarantul A and Müller A 2006 *Phys. Lett. A* **353** 48–59

[60] Tarantul A, Tsukerblat B and Müller A 2007 *Inorg. Chem.* **46** 161-169

[61] Tarantul A, Tsukerblat B and Müller A 2006 *Chem. Phys. Lett.* **428** 361–366

[62] Tsukerblat B, Tarantul A and Müller A 2006 *J. Chem. Phys* **125** 0547141

[63] Bates C A and Jasper R F, 1971 *J.Phys.C: Sol. State Phys.* **4** 2341 -53

[64] Varshalovich D A, Moskalev A N and Khersonskii V K 1988 *Quantum Theory of Angular Momentum* (Singapore: World Scientific)

[65] Gatteschi D, Sessoli R and Villain J 2006 *Molecular Nanomagnets* (Oxford: Oxford University Press)

[66] Bencini A and Gatteschi D 1990 *Electron Paramagnetic Resonance of Exchange Coupled Systems* (Berlin: Springer)
[67] Schnalle R and Schnack J 2010 *Int. Reviews in Physical Chemistry* **29** 403-452
[68] Van Vleck J H 1940 *Phys. Rev.* **57** 426-447
[69] Altshuler S A and Kozyrev B M 1974 *Electron Paramagnetic Resonance in Compounds of Transition Elements*, 2nd ed. (New York: Wiley)
[70] Orbach R 1961 *Proc. Roy. Soc.* **A254** (1319) 458-484
[71] Aminov L K 1962 *Sov. Phys. JETP* **15** 547
[72] Aminov L K 1974 *Zh. Exp. Teor. Phys.* **67** 79-83
[73] Aminov L K and Malkin B Z 2008 *Dynamics and Kinetics of Electronic and Spin Excitations in Paramagnetic Crystals (Russian)* (Kazan: Kazan State University)
[74] Heitler W 1957 *The Quantum Theory of Radiation* (Oxford: Clarendon Press)
[75] Tarantul A and Tsukerblat B 2010 *Inorg. Chim. Acta* **363** 4361-67
[76] Müller A and Döring J Private Communication
[77] Schlegel C, van Slageren J, Manoli M, Brechin E K and Dressel M 2009 *Polyhedron* **28** 1834-1837
[78] Belinsky M I 2008 *Inorg. Chem.* **47** 3521-31
[79] Belinsky M I 2008 *Inorg. Chem.* **47** 3532-39
[80] Kögerler P, Tsukerblat B and Müller A 2010 *Dalton Trans*. **39** 21–36